Smart minibots

DOI: 10.1002/smll.200800315

Biomimetic Soft Multifunctional Miniature Aquabots**

*Gu Han Kwon, Joong Yull Park, Jeong Yoon Kim, Megan L. Frisk, David J. Beebe, and Sang-Hoon Lee**

Engineered locomotive systems are widespread on the macro scale (e.g., planes, trains, automobiles), yet miniaturized mobile systems are largely limited to the research lab. In particular, integration of specific functions such as sensing or drug delivery into a small robot is a great challenge. The ability to miniaturize parts affecting motion, such as MEMS-based components and electroactive polymers, while widely demonstrated[1] has not led to practical advances in miniature multifunctional mobile robots. Rather complex construction, limits in the use of diverse materials, and cost (in case of the MEMS-based bot) all hinder the production of these robots. The small (micro-/millimeter scale) system within aqueous environments is particularly challenging, yet there are important potential applications for robots in such environments. To date, engineers have explored soft materials for creating components at the micro-/millimeter scales; for example, actuators such as ionic polymer metal composites, conducting polymers, and carbon nanotube actuators,[2–4] and engineered devices housing hydrogel valves, filters, and lenses[5–7], as well as other soft material actuators that mimic natural movement[8] (earthworm, myriapod, etc.). Still, the creation of miniature multifunctional robots that operate in aqueous environments has been elusive. Nature provides numerous examples of small, multifunctional and autonomous ''robots'' in the insect[9] and marine worlds after which we aimed to model miniature polymeric aquabots. Here we present mini (micro- to millimeter) soft aquabots that combine multiple functionalities to perform multifunctional operations in aqueous environments, effectively simulating their natural counterparts. Despite extensive research on macroscale robotics and miniature micro-electromechanical systems, relatively little attention has been paid to the creation of miniature soft robots with diverse shapes, actuation mechanisms, and integrated functionalities.

As a fabrication method, we describe a technique that takes advantage of the small volume required by a microfluidic chamber; this will be used for photopolymerizing multifunctional minibots that possess several ''organs,'' allowing for movement, sensing/signaling, and capture/transport/release. A diverse group of aquabots mimicking three kinds of living organisms – octopus, sperm, and myriapod, each representing a different mode of locomotion – has been developed. These aquabots have the following key features: 1) diverse shape and small size (sub-millimeter feature sizes); 2) a variety of functions (e.g., actuation, sensing) integrated in a single robot; and 3) rapid, scalable fabrication both in dimension and quantity. The aquabots were fabricated out of soft materials, due to the ease of polymerization, as well as the ability to tailor the material composition towards achieving certain functionality (e.g., responsiveness to pH, temperature, or electric/magnetic field). Sequential in situ photopolymerization within a microfluidic device allowed for precise fabrication of different components (arms, legs, body; see detailed procedure for photopolymerization in Experimental section). The bodies were constructed using a relatively inert polyethylene glycol (PEG) material, whereas ionic electroactive polymers (electroactive hydrogels)[10,11] were chosen from a large number of available soft materials to serve as the actuators, thus facilitating controlled movement. Depending on the application, some aquabots contained temperature-, pH-, or chemical-sensitive polymers in addition to their electroactive hydrogel and PEG components.

The gel network of polymerized actuator material was anionic, causing positively charged surfactant molecules to bind to its surface; this surfactant binding leads to an osmotic pressure difference between the gel interior and the external solution, thus inducing the contraction and curvature of the gel strip.[10,12] Four parameters control electroactive hydrogel-based actuators: 1) magnitude of the applied potential; 2) angle of the applied potential; and both 3) width and 4) length of the actuator. Figure 1A illustrates the behavior of a rectangular gel actuator under changing parameters (width of post and applied voltage; see Supporting Information Fig. S1 for more complete parameter characterization). In situ photopolymerization facilitates the control of the geometric parameters and is amenable to the use of laser or multiphoton polymerization methods for improved resolution (e.g., further reduce actuator width to achieve faster and larger motion).[13,14] To date, diverse electroactive hydrogels have been broadly applied to creating polymeric microactuators[15–19] (see the detailed behavior of electric-sensitive hydrogel in Supporting Information). Here, we demonstrate the use of electroactive hydrogel for fabricating octopus-, sperm-, and myriapod-like aquabots that retain respective characteristic movement (Fig. 2; movies are available for octopus-like aquabot and sperm-like aquabots in Supporting Information – Videos 1 and 2, respectively). The repeated bending test under aquatic conditions was carried out to investigate the durability of the electroactive hydrogel strips (see Supporting Information for a detailed durability test conditions). The operation of the

[*] Prof. S.-H. Lee, G. H. Kwon, Dr. J. Y. Park, Dr. J. Y. Kim
Department of Biomedical Engineering
College of Health Science, Korea University
Jeongneung-dong, Seongbuk-gu
Seoul 136-703 (Republic of Korea)
E-mail: dbiomed@korea.ac.kr
M. L. Frisk, Prof. D. J. Beebe
Department of Biomedical Engineering
University of Wisconsin-Madison
Madison, WI 53706 (USA)

[**] This study was supported by a grant from the Korea Health 21 R&D Project, Ministry of Health & Welfare, Republic of Korea (0405-ER01-0304-0001) and the NRL (National Research Lab) program, the Korea Science and Engineering Foundation (KOSEF), Republic of Korea (R0A-2007-000-20086-0).

Supporting Information is available on the WWW under http://www.small-journal.org or from the author.

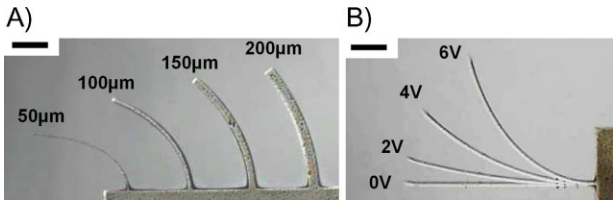

Figure 1. Actuation performance of hydrogel structure (4-HBA solution + PI (3.415 wt %)+CL (0.962 wt %) + AA (13.842 wt %)). A) Motion of hydrogel strip (*l*, 2 mm; *h*, 300 μm) with changing width, *w* (50, 100, 150, or 200 μm), in the presence of an applied voltage (+8 V). B) Motion of hydrogel strip (*l*, 4 mm; *h*, 300 μm; *w*, 100 μm) with changing applied voltage (0, 2, 4, or 6 V). Scale bars: 500 μm. (4-HBA: 4-hydroxy butyl acrylate; PI (photoinitiator): 2,2-dimethoxy-2-phenyl-acetophenone (DMPA); CL (crosslinker): ethylene glycol dimethacrylate (EGDMA); AA: acrylic acid.)

strip was stable and reproducible after 850 000 continuous bendings, indicating that the fabricated aquabots were very durable in aquatic conditions.

An octopus has an almost entirely soft body, with no internal skeleton, and moves either by jet propulsion (for brief sprints) or swimming (for slow sustained travel). The octopus aquabot mimics the swimming motion using a series of propelling and receding phases with four polymeric tentacles (Fig. 2A); during the receding phase, the application of a low voltage (+7 V) control signal causes all four tentacles to slowly bend upward – two clockwise (#1 and #2) and two counter-clockwise (#3 and #4) from their initial positions relative to a bisecting reference line. During the receding phase, all tentacles are bent upward to achieve propulsive power. Application of a high negative voltage (−15 V) at 4 s causes all four tentacles to realign downward, parallel with the reference line, thus resulting in rapid, upward propulsion of the octopus aquabot. An unbalanced control signal minimized backward movement during the receding phase. In total, the receding and propelling phases amounted to ≈5 s. The octopus aquabot demonstrated an instantaneous maximum speed of 5 mm s^{-1}, a mean speed of 0.76 mm s^{-1}, and a total distance travelled of 9.8 mm over the course of two upward propulsions (two receding/propelling cycles; Fig. 2B).

In addition to the octopus aquabot, a sperm-like aquabot consisting of a head and a single flagellum with dimensions of the order of 4 mm was developed; these dimensions are comparable to the lengths of actual sperm, that ranges

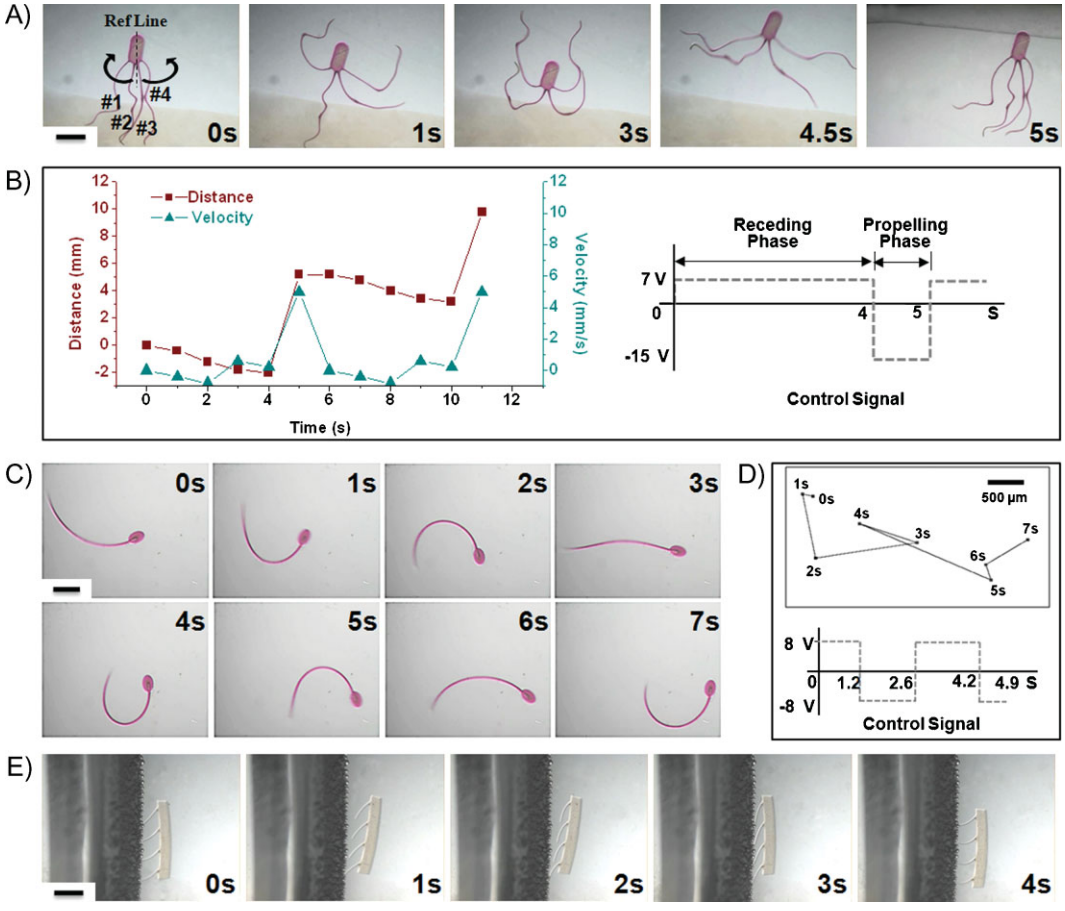

Figure 2. A) Locomotion of octopus aquabot under an electric field. Initial angles of tentacles 1 and 2 are each in the clockwise direction relative to the "Ref Line," while tentacles 3 and 4 are bent in the counter-clockwise direction. During the receding phase, all four tentacles were slowly bent upward, ready to propel; during the propelling phase, the aquabot rapidly moved upward by the propulsion of all four tentacles (scale bar = 1 mm). B) Velocity and distance profile for two periods with corresponding control signal (+7 V and −15 V were applied alternatively for different periods of time). C) Behavior of sperm aquabot with changing voltage (scale bar = 1 mm). D) Trajectory of sperm aquabot and corresponding control signal. E) Walking motion of myriapod aquabot with a mean translational speed of 0.125 mm s^{-1} (scale bar = 500 μm).

anywhere from 28 μm (porcupine sperm) to 5.8 cm (Drosophila bifurca sperm). In aqueous solutions, the aquabot flagellum oscillates in response to spatially alternating electrical control signals (Fig. 2C). Continuous application of the control signals results in a mean translational movement. The measured locomotion path of the sperm aquabot corresponded to maximum and mean speeds of 1.35 mm s^{-1} and 0.32 mm s^{-1}, respectively (Fig. 2D). In very low Reynolds number (*Re*) flow ($Re \ll 1$), the reciprocal motion of an object does not create any net movement. Therefore, at such small scales where viscous forces dominate, more effective propulsive mechanisms are utilized, such as the ''flexible oar'', ''cork screw'', and ''rotating flagellum''.[20,21] However, the scale of the sperm aquabot is of the order of a few millimeters and the typical *Re* is 1–10. This implies that inertial forces should be considered, and that temporal control will influence net motion; thus, the control of velocity is an integral factor in determining the resulting motion of the aquabot. Accordingly, when the control signal was symmetric, the bots did not produce net motion; when asymmetric control signals were applied (both amplitude and duration) net motion was observed for the sperm aquabot.

In order to demonstrate a nonswimming motion, a myriapod aquabot was created. Myriapoda is a subphylum of arthropods that includes millipedes, centipedes, and others – all of which are terrestrial and are characterized by numerous legs. Similarly, the myriapod aquabot consisted of a body and four legs (Fig. 2E). By alternating the control signal (±15 V), the myriapod aquabot slowly walked on a surface with a mean translational speed of 0.125 mm s^{-1}. Even though the bending angle of the individual myriapod legs was large, the translational distance per stroke was small because the legs did not bilaterally alternate like an actual myriapod (some legs used for forward movement, while other legs maintain stability). Instead, during the proceeding phase, the myriapod aquabot jumped slightly in the forward direction. Future work will focus on optimizing the control strategy and structural integrity in order to realize a myriapod-like walking mechanism.

Looking towards practical applications, several aquabots were fabricated that can be controlled using a mixture of electric and magnetic signals and include sensing/signalling or capture/transport/release functionalities. We report herein the development of various aquabots that can respond to environmental triggers (e.g., surface texture, chemical signals) or even capture – and subsequently deliver – targets, illustrating the versatility of aquabots. These ''applied'' aquabots have been divided into two broad categories based on their main functionalities – sensing and delivery.

In nature, the directionality of cells, bacteria, and other organisms is guided primarily by sensing chemical signals, as well as the topography of the surfaces with which they come into contact. We sought to add chemical responsiveness to the basic octopus aquabot. A glucose-sensing aquabot was fabricated. A glucose-responsive ''eye'' was incorporated into the body of the octopus aquabot using immobilizing horseradish peroxidase (HRP) and glucose oxidase (GOx). Upon exposure to a solution containing glucose and Amplex Red, glucose is broken down and releases H_2O_2 which, in combination with HRP, converts Amplex Red to a fluorescent product that can be detected with fluorescence microscopy (Fig. 3A). Lastly, rather than rely on a fluorescent readout – which can be complicated by expensive instrumentation – a sensor based on gel degradation was incorporated using either a disulfide-crosslinked polymer or a trypsin-sensitive peptide crosslinker as the aquabot ''head.'' When the octopus aquabot was exposed to a reducing agent for a short period of time (≈10 min), the disulfide-crosslinked gel dissolved (Fig. 3B). Similarly, when the peptide-crosslinked head was exposed to a trypsin solution, the polymer degraded within 30 min (Fig. 3C). In the latter case, fluorescent beads were co-photopolymerized with the peptide gel to form the octopus head; upon degradation, the beads were released and were able to diffuse into surrounding areas, simulating a ''drug delivery'' concept. Polymer degradation in response to a specific stimulus (in this case dithiothreitol or trypsin) mimics a drug delivery situation, in which the drug would be housed in the gel, only to be released upon exposure to a chosen stimulus, as demonstrated in Figure 3B and C.

Lastly, delivery aquabots were designed for facile repositioning of small targets. Magnetically movable delivery aquabots were fabricated with three different means of controlling the ''arms'' – the major component that facilitated movement of a target object, in this case a PEG disc. The magnetic body of all three delivery aquabots consisted of body material with embedded nickel nanoparticles, rendering them susceptible to precise motion control with an external magnet. First, two electroactive hydrogel arms were attached to the top of the magnetic aquabot body. Figure 3D shows the aquabot grabbing the circular target (disc shape) upon application of an electric field (+8 V) and then moving to a specific position via magnetic control. Upon turning off the power, the aquabot released the target. A pH-responsive delivery aquabot was then fabricated with hydroxyethyl methacrylate (HEMA) arms and a magnetic body; its behavior in different pH solutions as a function of time is illustrated in Figure 3E. In an acidic solution (pH ≈ 3), the arms shrunk and the aquabot was magnetically maneuvered toward the target. In basic solution (pH ≈ 10), the legs swelled, causing the aquabot to hold the target as it was dragged to a designated position. Upon reintroduction of an acidic solution, the target was released. Finally, a temperature-responsive delivery aquabot was developed with N-isopropylacrylamide (NIPAAm) arms that expanded at lower temperatures (≈25 °C) and contracted at higher temperatures (≈45 °C), allowing for capture and release of the target (Fig. 3F). It is therefore evident that different soft materials can be employed to achieve similar functionality in a variety of environments. Importantly, the capture and release function is autonomously triggered by the inherent properties of the local environment.

In summary, miniature aquabots were successfully fabricated using microfluidic chambers and sequential in situ photopolymerization. The integration of appropriate soft polymers allowed for diverse capabilities including locomotion, sensing/signaling, and transport/capture/release. We have demonstrated a simple fabrication technique that uses a combination of stimuli-responsive and non-responsive polymers for realizing miniature aquabots that exhibit a range

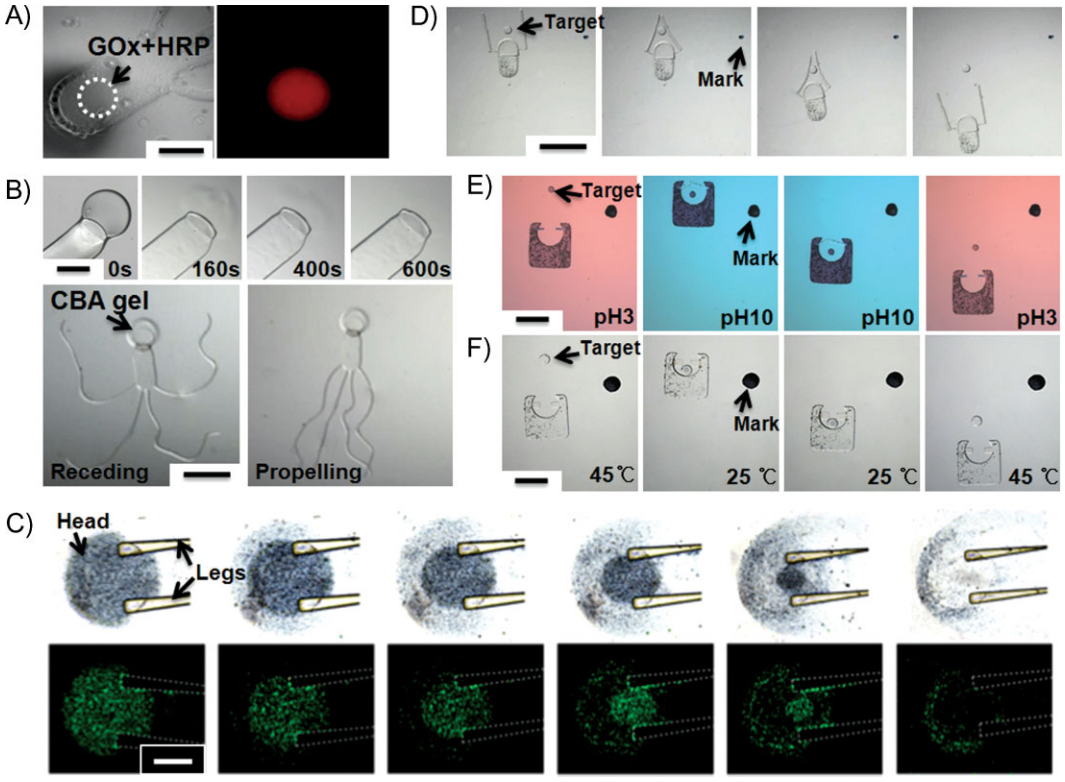

Figure 3. Stimuli-responsive aquabots. A) Glucose-responsive aquabot fabricated with an eye containing immobilized HRP and GOx (left) that, in the presence of glucose and Amplex Red, fluoresces (right) (scale bar = 500 μm). B) Chemical-responsive drug delivery aquabot with a DTT-sensitive CBA (cysteamine bisacrylamide) gel head that completely dissolves when exposed to a DTT solution for 10 min (scale bar = 500 μm). C) Chemical-responsive drug delivery aquabot with a trypsin-sensitive SNAP gel head that completely dissolves when exposed to a trypsin solution for 30 min; phase and fluorescent images were taken (scale bar = 500 μm). D) Electro-responsive carrier aquabot containing nickel nanoparticles (black area of body) carries out translational movement caused by an external magnetic field. When this aquabot is exposed to an electric field, the arms grab the spherical target (scale bar: 1 mm). E) pH-responsive carrier aquabot possesses HEMA legs that shrink at acidic pH (≈3) and swell at basic pH (≈10). Using this expansion/contraction mechanism, the aquabot can catch, drag (using an external magnet), and release a target (scale bar = 1 mm). F) Temperature-responsive carrier aquabot that performs similarly to the pH-responsive aquabot, but is fabricated with NIPAAm temperature-sensitive legs (scale bar = 1 mm).

of diverse functionalities. Diffusion-based actuation scales favorably, leading to practical actuation speed and force combinations. The ability of these aquabots to perform various functions while mimicking the movement of living organisms (octopus, sperm, and myriapod) in aqueous environments suggests their potential use in the biological, biomedical and other various fields (e.g., medical diagnosis, drug delivery, or environmental monitoring and inspection).

Using laser, multiphoton, and grayscale polymerization methods,[22] one can envision truly three-dimensional aquabots with expanded functionality. In addition, oscillating gels[23] might enable locomotion without the spatial constraints of electrical actuation, thus resulting in free-roaming aquabots. The requirement for external control of magnetically and electrically operable polymers could be leveraged in applications such as minimally invasive tools for disease diagnosis, drug delivery, or environmental monitoring and inspection. For example, stimuli-responsive polymers have been developed that can easily be incorporated into existing aquabot structures (PEG body or electroactive hydrogel actuators) for creating miniature bots capable of sensing a particular analyte.[24] Aquabots with sensor/payload heads (similar to the trypsin-sensitive head) could sense specific organisms and destroy them, preventing the spread of invasive species.

Experimental Section

Materials: Horseradish peroxidase (HRP, EC 1.11.1.7, 330 units mg^{-1}), glucose oxidase from *Aspergillus niger* (GOx, EC 1.1.3.4,47.2 units mg^{-1}), trypsin, Rhodamine B, and magnetic agarose beads (≈40 μm) were purchased from Sigma (St. Louis, MO, USA). Yellow-green carboxy-modified 2.0 μm FluoSpheres® 505/515 (2% w v^{-1} in distilled water with 2 mM sodium azide) and *N*-acetyl-3,7-dihydroxyphenoxazine (Amplex Red) were purchased from Molecular Probes (Eugene, OR, USA). Poly(dimethylsiloxane) (PDMS) was purchased from Dow Corning Co. (Midland, MI, USA). Poly(ethylene glycol) diacrylate (PEG-DA), 4-hydroxybutyl acrylate (4-HBA), 2-hydroxyethyl methacrylate (HEMA), *N*-isopropylacrylamide (NIPAAm), 2,2-dimethoxy-2-phenylacetophenone (DMPA), ethylene glycol dimethacrylate (EGDMA), isobornyl acrylate (IBA), *N*-methylenebisacrylamide (NMBA), sodium chloride (NaCl), sodium dihydrogen phosphate (NaH_2PO_4), trifluoroacetic acid

(TFA), and acrylic acid (AA) were purchased from Aldrich (St. Louis, MO, USA) and were used as received. Thioanisole was obtained from Acros Organics. Ethanedithiol (EDT) was obtained from Alfa Aesar. 4-(2-hydroxyethyl)-1-piperazineethanesulfonic acid (HEPES) and phosphate buffered saline (10X, PBS) was purchased from Fisher Scientific. Tetra(ethylene glycol) dimethacrylate (TeEGDMA) was obtained from Fluka. *N*,*N*′-cystamine-bis-acrylamide was obtained from MP Biomedicals. (*N*-[2-(2-pyridyldithio)]ethyl methacrylamide) (PDTEMA) was synthesized in the Moore lab at University of Illinois at Urbana-Champaign according to a previously published protocol[25] and then generously provided for our experiments. Most of the figures were imaged on a fluorescence microscope (Axiovert 200M, Cal Zeizz, Germany) and a stereoscope (Olympus SZ61, Olympus, Janpan). Figure 3G was imaged on an Olympus BX60 with a Leica DFC 300 camera; all phase images were retouched with Adobe Photoshop CS v8.0 to remove large scratches apparent on the polycarbonate cover of that particular microfluidic chamber.

Aquabot Fabrication: Sequential in situ photopolymerization method based on a microfluidic platform was employed. A PDMS-based microfluidic device (channel size 7 mm $\times$5 mm $\times$300 μm) was prepared with a glass cover. A special aligning apparatus was designed to hold the microfluidic device as shown in Figure 4. The aligning apparatus consisted of an automatic aligning system (translational resolution to x- and y-axes was less than 5 μm each), which was used to align the photomask with the fiduciary mark on the PDMS platform and the UV lamp with a focusing lens for accurate transfer of photomask patterns. Prepolymer solution was introduced via syringes directly connected to the PDMS micro device. UV radiation through a photomask (designed in AutoCAD and printed on transparency film) allowed for facile patterning of hydrogel structures inside the microfluidic chamber. Unpolymerized material was washed out with PBS. Multiple structures could be formed in this manner, thus demonstrating sequential in situ photopolymerization.

To initially verify the aligning capability of this device, the gelled 'Mickey Mouse' with a total size of 2 mm was fabricated (Fig. 4B). The hydrogel prepolymer mixed with either red (for tongue and background), black (head, eye, nose, and body), or yellow dye (face) was introduced, polymerized by UV light radiated through the photomask, and finally washed with water. The aquabots were also polymerized using this microfluidic/aligning apparatus and, when all necessary structures were polymerized, the cover glass was separated from the PDMS to "release" the aquabot. Figure 4C displays the polymerized octopus aquabot on the surface of the cover glass. It is difficult to separate the aquabot from the cover glass as the thin tentacles can be broken by slight stress. For ease of detachment, water was dropped on the polymerized octopus aquabot, which allowed the body and tentacles to swell, therefore forcing separation. Figure 4C illustrates the tentacles' separation process over time (1–3 min). Finally, the body of the octopus could be easily detached by scratching with a sharp razor blade. The entire process required $\approx$10 min.

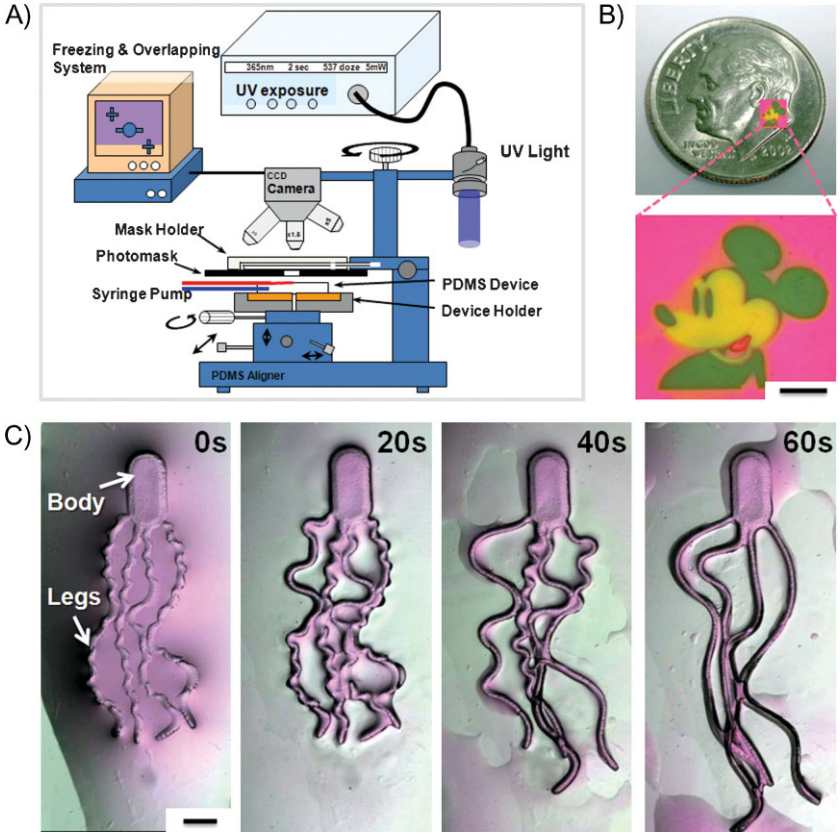

Figure 4. Experimental setup and photopolymerization. A) Schematic diagram of automatic aligning system for the sequential in situ hydrogel-based micropatterning. B) Gelled 'Mickey Mouse' created using sequential in situ photopolymerization; each component contained PEG-DA and necessary monomers and photoinitiators (inset: the separated 'Mickey Mouse' (noted by arrow) on the dime; scale bar: 500 μm). C) Octopus aquabot on the cover glass (pink color represents Rhodamine B) after polymerization. Autonomous detachment of aquabot from the cover glass by adding water (after 20 s, thin tentacles begin to separate due to rapid swelling; scale bar: 500 μm).

Keywords:

biomimetics · electroactive hydrogels · microengineering · minibots · polymers

[1] S. Collins, A. Ruina, R. Tedrake, M. Wisse, *Science* **2005**, *307*, 1082.
[2] P. Arena, C. Bonomo, L. Fortuna, M. Frasca, S. Graziani, *IEEE Trans. Syst. Man Cybern. B* **2006**, *36*, 1044.
[3] Y. Yun, V. Shanov, Y. Tu, M. J. Schulz, S. Yarmolenko, S. Neralla, J. Sankar, S. Subramaniam, *Nano Lett.* **2006**, *6*, 689.
[4] J. Casanovas, D. Zanuy, C. Aleman, *Angew. Chem. Int. Ed.* **2006**, *45*, 1103.
[5] J. Y. Park, H. J. Oh, D. J. Kim, J. Y. Baek, S. H. Lee, *J. Micromech. Microeng.* **2006**, *16*, 656.
[6] D. Kim, D. J. Beebe, *Lab Chip* **2007**, *7*, 193.
[7] L. Dong, A. K. Agarwal, D. J. Beebe, H. R. Jiang, *Nature* **2006**, *442*, 551.

[8] L. Yeghiazarian, H. Arora, V. Nistor, C. Montemagno, U. Wiesner, *Soft Matter* **2007**, *3*, 939.
[9] T. Eisner, *For Love of Insects*, Belknap Press of Harvard University Press, Cambridge, MA 2003.
[10] Y. Osada, H. Okuzaki, H. Hori, *Nature* **1992**, *355*, 242.
[11] Y. Bar-Cohen, *Strain* **2005**, *41*, 19.
[12] Y. K. M. Otake, Y. Kuniyoshi, M. Inaba, H. Inoue, presented at IEEE International Conference of Robotics & Automation, Washington, DC, USA, May 2002.
[13] S. Song, A. K. Singh, B. J. Kirby, *Anal. Chem.* **2004**, *76*, 4589.
[14] S. Kawata, H. B. Sun, T. Tanaka, K. Takada, *Nature* **2001**, *412*, 697.
[15] E. W. H. Jager, O. Inganas, I. Lundstrom, *Science* **2000**, *288*, 2335.
[16] E. Smela, O. Inganas, I. Lundstrom, *Science* **1995**, *268*, 1735.
[17] R. Pelrine, R. Kornbluh, Q. B. Pei, J. Joseph, *Science* **2000**, *287*, 836.
[18] Q. M. Zhang, H. F. Li, M. Poh, F. Xia, Z. Y. Cheng, H. S. Xu, C. Huang, *Nature* **2002**, *419*, 284.
[19] R. Dreyfus, J. Baudry, M. L. Roper, M. Fermigier, H. A. Stone, J. Bibette, *Nature* **2005**, *437*, 862.
[20] E. M. Purcell, *Am. J. Phys.* **1977**, *45*, 3.
[21] E. M. Purcell, *Proc. Natl. Acad. Sci. USA* **1997**, *94*, 11307.
[22] C. C. Chen, D. Hirdes, A. Folch, *Proc. Natl. Acad. Sci. USA* **2003**, *100*, 1499.
[23] R. Yoshida, T. Takahashi, T. Yamaguchi, H. Ichijo, *J. Am. Chem. Soc.* **1996**, *118*, 5134.
[24] M. L. Frisk, W. H. Tepp, G. Lin, E. A. Johnson, D. J. Beebe, *Chem. Mater.* **2007**, *19*, 5842–5844.
[25] L. Wang, J. Kristensen, D. E. Ruffner, *Bioconjugate Chem.* **1998**, *9*, 749.

Received: February 20, 2008
Revised: April 24, 2008
Published online: November 6, 2008

